



Trans. Nonferrous Met. Soc. China 22(2012) 793-802

Transactions of Nonferrous Metals Society of China

www.tnmsc.cn

# Corrosion behaviour of friction stir welded AZ61A magnesium alloy welds immersed in NaCl solutions

A. DHANAPAL<sup>1</sup>, S. RAJENDRA BOOPATHY<sup>2</sup>, V. BALASUBRAMANIAN<sup>3</sup>

- 1. Department of Mechanical Engineering, Sri Ramanujar Engineering College, Vandalur, Chennai – 600 048, Tamil Nadu, India;
- 2. Department of Mechanical Engineering, College of Engineering, Guindy, Anna University, Chennai 600 025, Tamil Nadu, India;
- 3. Center for Materials Joining & Research (CEMAJOR), Department of Manufacturing Engineering, Annamalai University, Annamalainagar 608 002, Chidambaram, Tamil Nadu, India

Received 30 June 2011; accepted 19 September 2011

**Abstract:** The extruded AZ61A magnesium alloy plates of 6 mm thickness were butt welded using friction stir welding (FSW) process. The corrosion behavior of the welds was evaluated by conducting immersion test in NaCl solution at different pH value, immersion time and chloride ion concentrations. An empirical relationship was established incorporating pH value, immersion time and chloride ion concentration to predict the corrosion rate of friction stir welds of AZ61A magnesium alloy at 95% confidence level. Three-factor, five-level central composite rotatable design was used to minimize the number of experimental conditions. Response surface method was used to develop the relationship. The results show that the corrosion resistance of AZ61A magnesium alloy welds in the alkaline solution is better than that in the acidic and neutral solutions, moreover, low corrosion rate is found at low concentrated solution and longer exposure time, and the corrosion morphology is predominantly influenced by the distribution of β-phase.

Key words: magnesium alloy; immersion corrosion; friction stir welding

### 1 Introduction

The desire to use lightweight metallic alloy in the automotive, aerospace and electronic industries has increased in recent years as the search for lightweight materials has been amplified [1,2]. Magnesium alloy is one of these lightweight metallic alloys currently being investigated, for its many excellent properties such as low density, high specific strength, high thermal conductivity and its resistance to electromagnetic interference [3]. The benefits of magnesium, however, are contrasted by high corrosion rate as compared to aluminium or steel, because of magnesium's electrochemical potential as illustrated in the presence of seawater [4]. The high corrosion of magnesium has regulated the alloy to be used in areas unexposed to the atmosphere, including car seats and electronic boxes [5,6].

The application of Mg alloy in structural members

is still limited due to many solidification related problems such as hot cracking, porosity, alloy segregation and partial melting zone occurred during fusion welding. To avoid these problems, friction stir welding (FSW) process can be used. FSW is a solid state welding process without emission of radiation or dangerous fumes, and it avoids the formation of solidification defects like hot cracking and porosity. Moreover, it significantly improves the weld properties and hence is extensively applied to joining magnesium alloys [7].

Immersion testing that is the main technique for corrosion studies was employed in this research in an effort to expose the AZ61 Mg alloy to an environment similar to that experienced by automotive engine blocks [8]. The pH of test solution had a considerable effect on the corrosion rate of Mg. However, it is difficult to keep it consistent, especially in a neutral solution because the corrosion product of Mg, Mg(OH), readily dissolves into the solution, which results in substantial increase in the

pH value [9]. The electrochemical behavior of Mg–11Li–3Al–0.5 RE was studied with the use of potentiodynamic polarization curves and electrochemical impendence. The alloy exhibited an increased corrosion rate with the increasing chloride ion concentration [10].

In a buffer chloride solution, the corrosion rate of magnesium and its alloy did not depend on their purity or the content of the major alloying elements, but solely on the pH value of the solution [11]. Magnesium can quickly develop an oxide film on the surface in air, but this oxide MgO, with Pilling-Bedworth ratio 0.81 can only provide limited protection [12]. The thickness of the oxide film formed on the surface of the specimen increased with the increase of pH [13]. The corrosion rate of AZ91 was higher in acidic solution than in a neutral or highly alkaline solution. Here, the mode of corrosion was pitting. Large pits were formed as the corrosion pits expanded towards the inner matrix and enlarged all around [14]. The general and pitting corrosion behavior of parent and FSW nugget regions were nearly the same, even though they were different in the untreated condition. The corrosion morphology of the AM50 alloy was predominantly controlled by the  $\beta$ -phase distribution. Pitting corrosion was discerned in the welds [15,16].

From the literature review, it is understood that most of the published information on corrosion behavior of Mg alloys was focused on pitting corrosion and general corrosion of the unwelded base alloys. Hence, the present investigation was carried out to study the corrosion behavior of AZ61A magnesium alloy welds. Also an empirical relationship was developed to predict the corrosion rate of friction stir welds of AZ61A Mg alloy under immersion conditions.

# 2 Experimental

#### 2.1 Materials

The material used in this study was AZ61A magnesium alloy in the form of extruded plates of 6 mm thickness. The chemical composition and mechanical properties of the base metal are presented in Tables 1 and 2. The optical micrograph of the base metal is shown in Fig. 1. The plate was cut into a required size (300 mm×150 mm) by power hacksaw followed by milling. The square butt joint configuration was prepared to fabricate the joints. The initial joint configuration was obtained by securing the plates in position using mechanical clamps. The direction of welding was normal to the extruded direction. Single pass welding procedure was followed to fabricate the joints. A non-consumable tool made of high carbon steel was used to fabricate the

joints. An indigenously designed and developed computer numerical controlled friction stir welding (22 kW; 4000 r/min; 60 kN) was used to fabricate the joints. The FSW parameters were optimized by conducting trial runs and the welding conditions which produced defect-free joints were taken as the optimized welding conditions. The optimized welding conditions used to fabricate the joints in this investigation are presented in Table 3.

**Table 1** Chemical composition of AZ61A Mg alloy (mass fraction, %)

Al	Zn	Mn	Mg
5.45	1.26	0.17	Bal.

Table 2 Mechanical properties of AZ61A Mg alloy

			<u> </u>
Yield	Ultimate tensile	Elongation/	Vickers hardness at
strength/MPa	strength/MPa	%	0.5 N load (HV)
176.49	271.68	8.40	56.3

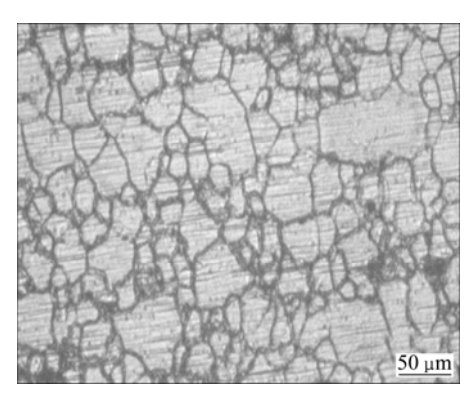


Fig. 1 Optical micrograph of AZ61A base metal

**Table 3** Optimized welding conditions and process parameters used to fabricate joints

Parameter	Value				
Rotational speed/ $(r \cdot min^{-1})$	1000				
Welding speed/(mm·min <sup>-1</sup> )	75				
Axial force/kN	3				
Tool shoulder diameter/mm	18				
Pin diameter/mm	6				
Pin length/mm	5				
Pin profile	Left hand thread of 1 mm pitch				

From the welded joints, the corrosion test specimens were extracted from the friction stir welds with the dimensions of 50 mm×16 mm×6 mm, as shown in Fig. 2. The specimens were ground with 500<sup>#</sup>, 800<sup>#</sup>, 1200<sup>#</sup> and 1500<sup>#</sup> grit SiC paper. Finally, they were cleaned with acetone and washed in distilled water, and then dried by warm flowing air. The optical micrograph of the friction stir weld region is shown in Fig. 3.

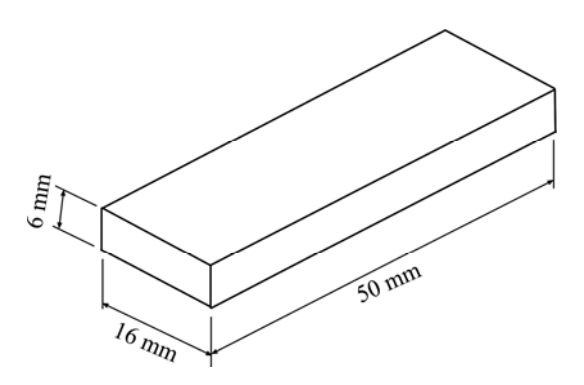


Fig. 2 Dimensions of corrosion test specimen

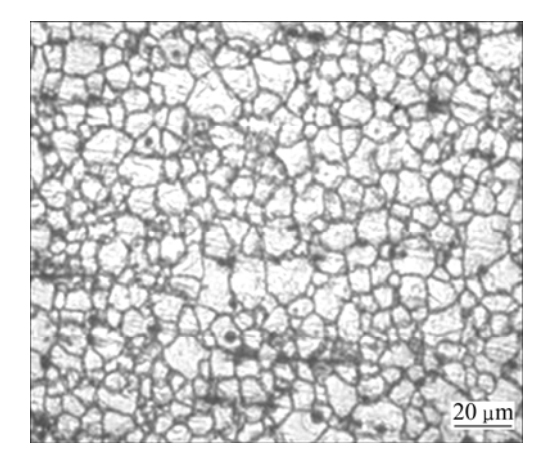


Fig. 3 Optical micrograph of friction stir weld region

#### 2.2 Limits of corrosion test parameters

From Refs. [17,18], the predominant factors that have great influence on the corrosion behavior of AZ61A magnesium alloy are identified. They are pH value of the solution, immersion time, and chloride ion concentration. Large number of trial experiments were conducted to identify the feasible testing conditions for the friction stir welded AZ61A magnesium alloy weld metal region under immersion conditions. The following inferences are obtained:

- 1) If pH value of the solution was less than 3, the change in chloride ion concentration did not considerably affect the corrosion.
- 2) If the pH value was between 3 to 11, an inhibition of the corrosion process would occur due to the protective layer.
- 3) If pH value was greater than 11, blocking of further corrosion by the active centers of protective layer took place.
- 4) If the chloride ion concentration was less than 0.2 mol/L, visible corrosion did not occur in the experimental period.
- 5) If the chloride ion concentration was between 0.2 to 1 mol/L, there was a reasonable fluctuation in the corrosion rate.

- 6) If the chloride ion concentration was greater than 1 mol/L, the corrosion rate might hesitate and decrease a little.
- 7) If the immersion time was less than 1 h, the surface was completely covered with the thick and rough corrosion products and had an unpredicted corrosion rate.
- 8) If the immersion time was between 1 to 9 h, the tracks of the corrosion could be predicted.
- 9) If the immersion time was longer than 9 h, the tracks of corrosion film were difficult to identify.

#### 2.3 Experimental design matrix

Owing to a wide range of factors, the method of three factors and central composite rotatable design matrix was chosen to minimize the number of experiments. Design matrix consisting of 20 sets of coded conditions (composing a full replication three factorial of 8 points, 6 corner points and 6 centre points) was chosen in this investigation. Table 4 presents the ranges of factors considered, and Table 5 shows the 20 sets of coded and actual values used to conduct the experiments.

**Table 4** Important factors and their levels

Factor	Notation	Unit	Level				
	Notation	Omt	-1.682	-1	0	+1	+1.682
pH value	P		3	4.62	7	9.38	11
Immersion time	t	h	1	2.62	5	7.38	9
Cl <sup>-</sup> concentration	c	mol/L	0.20	0.36	0.60	0.84	1

For the convenience of recording and processing the experimental data, the upper and lower levels of the factors were coded here as +1.682 and -1.682, respectively. The coded values of any intermediate value could be calculated using the following relationship:

$$X_i = 1.682[2X - (X_{\text{max}} - X_{\text{min}})]/(X_{\text{max}} - X_{\text{min}})$$
 (1)

where  $X_i$  is the required coded value of a variable X and X is any value of the variable from  $X_{\min}$  to  $X_{\max}$ ;  $X_{\min}$  is the lower level of the variable;  $X_{\max}$  is the upper level of the variable.

# 2.4 Responses

The corrosion rate of the friction stir welded AZ61A alloy specimen was estimated by mass loss measurement under immersion tests as per ASTM G31—72. The original mass ( $m_0$ ) of the specimen was recorded and then the specimen was immersed into the solution of NaCl for different immersion time of 1, 2.62, 5, 7.38 and 9 h. Finally, the corrosion products were removed by immersing the specimens for 1 min in a solution

**Table 5** Design matrix and experimental results

М		Coded value	oded value		Actual value	;	C 1
No	pН	Time	Conc.	рН	Time/h	Conc/(mol·L <sup>-1</sup> )	Corrosion rate/(mm·a $^{-1}$ )
1	-1	-1	-1	4.62	2.62	0.36	6.32 (0.12)
2	+1	-1	-1	9.38	2.62	0.36	4.62 (0.58)
3	-1	+1	-1	4.62	7.38	0.36	4.63 (0.74)
4	+1	+1	-1	9.38	7.38	0.36	3.99 (0.21)
5	-1	-1	+1	4.62	2.62	0.84	9.60 (0.2)
6	+1	-1	+1	9.38	2.62	0.84	5.62 (0.08)
7	-1	+1	+1	4.62	7.38	0.84	8.43 (0.04)
8	+1	+1	+1	9.38	7.38	0.84	6.65 (0.05)
9	-1.682	0	0	3	5	0.60	6.60 (0.21)
10	+1.682	0	0	11	5	0.60	4.65 (0.27)
11	0	-1.682	0	7	1	0.60	6.21 (0.21)
12	0	+1.682	0	7	9	0.60	4.36 (0.38)
13	0	0	-1.682	7	5	0.20	6.45 (0.51)
14	0	0	+1.682	7	5	1.0	8.95 (0.13)
15	0	0	0	7	5	0.60	4.56 (0.16)
16	0	0	0	7	5	0.60	5.54 (0.12)
17	0	0	0	7	5	0.60	4.57 (0.28)
18	0	0	0	7	5	0.60	4.61 (0.26)
19	0	0	0	7	5	0.60	4.66 (0.01)
20	0	0	0	7	5	0.60	4.85 (0.10)

<sup>\*</sup>The values presented in bracket are standard deviation

prepared by using 50 g chromium trioxide (CrO<sub>3</sub>), 2.5 g silver nitrate (AgNO<sub>3</sub>) and 5 g barium nitrate(Ba(NO<sub>3</sub>)<sub>2</sub>) in 250 mL distilled water. These specimens were washed with distilled water, dried and weighed again to obtain the final mass  $(m_1)$ . The mass loss  $(\Delta m)$  could be obtained using the following relation:

$$\Delta m = m_0 - m_1 \tag{2}$$

The corrosion rate (R) of FSW weld metal region can be calculated using the following equation by conducting the immersion test as per ASTM standards G1-03.

$$R = \frac{8.76 \times 10^4 \times \Delta m}{A \times D \times t} \tag{3}$$

where R is the corrosion rate in mm/a; A is the surface area of the specimen in cm<sup>2</sup>; D is the density of the material, 1.72 g/cm<sup>3</sup>; t is the corrosion time in hour.

Microstructural analysis was carried out on the corroded specimens using a light optical microscope (Make: Union Opt. Co. Ltd. Japan; Model: VERSAMET-3) incorporated with an image analyzing software (Clemex-vision). The exposed specimen surface was prepared for the micro examination both in the "AS polished" and "AS etched" conditions. Picral+acetic acid

was used as etchant. The corrosion test specimens were polished in disc polishing machine for scratching fewer surfaces and the surface was observed at 200X magnification.

#### 3 Development of empirical relationship

In the present investigation, to correlate the immersion test parameters and the corrosion rate of welds, a second order quadratic model was developed. The response (corrosion rate) is a function of pH value (P), immersion time (t) and chloride ion concentration (c) which can be expressed as:

$$R = f(P, t, c) \tag{4}$$

The empirical relationship must include the main and interaction effects of all factors and hence the selected polynomial is expressed as follows:

$$Y = b_0 + \sum b_i X_i + \sum b_{ii} X_i^2 + \sum b_{ij} X_i X_j$$

$$\tag{5}$$

For three factors, the selected polynomial can be expressed as:

$$R = b_0 + b_1 P + b_2 t + b_3 c + b_{11} P^2 + b_{22} t^2 + b_{33} c^2 + b_{12} P t + b_{13} P c + b_{23} t c$$

$$(6)$$

where  $b_0$  is the average of responses (corrosion rate) and

 $b_1$ ,  $b_2$ ,  $b_3$ ,  $b_{11}$ ,  $b_{12}$ ,  $b_{13}$ ,  $b_{22}$ ,  $b_{23}$ ,  $b_{33}$  are the coefficients that depend on the respective main and interaction factors, which are calculated using the expression given below,

$$b_i = \sum (X_i Y_i)/n \tag{7}$$

where i varies from 1 to n,  $X_i$  is the corresponding coded value of a factor and  $Y_i$  is the corresponding response output value (corrosion rate) obtained from the experiment and n is the total number of combination considered. All the coefficients were obtained by applying central composite rotatable design matrix using the Design Expert statistical software package. After determining the significant coefficients (at 95% confidence level), the final relationship was developed including only these coefficients. The final empirical relationship obtained by the above procedure to estimate the corrosion rate of friction stir welds of AZ61A magnesium alloy is given as:

$$R=4.81-0.83P-0.41t+1.09c+0.41Pt-0.43Pc+0.28P^2+1.019c^2$$
(8)

The analysis of variance (ANOVA) technique was used to find the significant main and interaction factors. The results of second order response surface model fitting as ANOVA are given in Table 6. The determination coefficient ( $r^2$ ) indicates the goodness of fit for the model. The Model F-value of 31.30 infers that the model is significant. There is only a 0.01% chance that a "Model F-Value" could occur due to noise [19].

Table 6 ANOVA test results

Source	Sum of square	df	Mean square	F-value	p-value Prob> <i>F</i>	_
Model	26.16	9	2.91	29.22	< 0.0001	Significant
P	2.76	1	2.76	27.7	0.0004	
t	19.41	1	19.41	195.19	< 0.0001	
С	1.08	1	1.08	10.88	0.0080	
Pt	0.65	1	0.65	6.54	0.0285	
Pc	0.097	1	0.097	0.98	0.3461	
tc	0.49	1	0.49	4.93	0.0507	
$P^2$	0.24	1	0.24	2.39	0.1534	
$t^2$	1.22	1	1.22	12.23	0.0057	
$c^2$	0.056	1	0.056	0.57	0.4686	
Residual	0.099	10	0.099			
Lack of fit	0.62	5	0.12	1.63	0.3036	Not significant
Pure error	0.38	5	0.076			
Cor total	27.15	19				

The values of "Prob>F" less than 0.0500 indicate that the model terms are significant. In this case, P, t, c, Pt, tc and  $t^2$  are significant model terms. The values greater than 0.1000 indicate that the model terms are not

significant. If there are many insignificant model terms (not counting those required to support hierarchy), model reduction may improve your model. The "Lack of fit F-value" of 3.03 implies that the "Lack of fit" is not significant relative to the pure error. There is a 12.47% chance that a "Lack of fit F-value" could occur due to noise. All these indicate an excellent suitability of the regression model. Each of the observed values was compared with the experimental values, as shown in Fig. 4 [20,21]. A scatter plot of the two variables indicates that a straight line should provide an excellent fit to the data. The differences between the actual and predicted responses are termed as residuals. The residuals provide a measure of the closeness of agreement of the actual and the predicted responses. Hence, they provide a measure of the adequacy of the fitted model. The difference in the actual and the predicted responses is clearly shown in Fig. 4. The linear fit approximates the observed data points so well; the residuals obtained from the ANOVA test results are very low as shown in Table 6. The distance between the true line (black line) and the dotted lines is the residual. Small residuals are one important indicator of the adequacy of a regression fit.

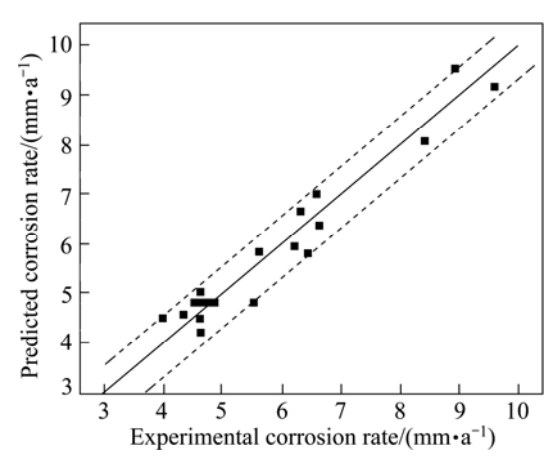


Fig. 4 Correlation graph for response

To validate the developed model, three confirmation experiments were carried out with the process parameters chosen randomly close to the range of experimental parameters. For the actual responses the average of three measured was calculated. Table 7 summarizes the

Table 7 Validation of test results

No. pH		Exposure time/h	Cl <sup>-</sup> ion Conc./	Cor rate/(	Error/	
		tillie/ li	$(\text{mol} \cdot \text{L}^{-1})$	Actual	Predicted	/0
1	4	2	0.4	6.4	6.51	1.7
2	8	6	0.8	4.3	4.417	2.7
3	6	4	0.6	3.62	3.653	1.4

experimental condition, the average actual values, the predicted values and the error. The optimum values of process parameters and the corrosion rate of friction stir welded AZ61A magnesium alloy welds show excellent agreement with the predicted values.

#### 4 Results and discussion

Table 5 shows the corrosion rates obtained from immersion test as a function of pH, immersion time and chloride ion concentration. At all pH values, the friction stir welded metal exhibited a rise in corrosion rate with the decrease in pH value. In the neutral pH, the corrosion rate remained constant approximately and a comparatively low corrosion rate was observed in alkaline solutions. Furthermore, it was seen that the influence of pH was more at higher concentration as compared to at lower concentrations in neutral and alkaline solutions. It was also observed that the corrosion rate of friction stir welded AZ61A Mg alloy was quite comparable with the corrosion rate of the referred

articles of same series of magnesium alloys [22,23].

Figure 5 shows the corrosion morphology and pit morphology of the corroded specimen after immersion tests at pH 3, 7 and 11 with constant chloride ion concentration of 0.60 mol/L and immersion time of 5 h respectively. It is seen that, at a lower concentration of chloride ion, the surface of the specimen was relatively slightly corroded in neutral or alkaline solutions while was severely corroded at all pH values at a higher concentrations of chloride ion. The corrosion of FSW weld metal region was significantly influenced by pH value. The dissolution of magnesium in aqueous solutions proceeded by the reduction of water to produce magnesium hydroxide Mg(OH)<sub>2</sub> and hydrogen gas (H<sub>2</sub>). The reduction process was primarily water reduction. These reactions were reported to be insensitive to oxygen concentration.

$$Mg \rightarrow Mg^{2+} + 2e^{-} \tag{9}$$

$$2H_2O + 2e^{-} \rightarrow 2OH^{-} + H_2 \tag{10}$$

$$Mg^{2+} + 2OH^{-} \longrightarrow Mg(OH)_{2}$$
 (11)

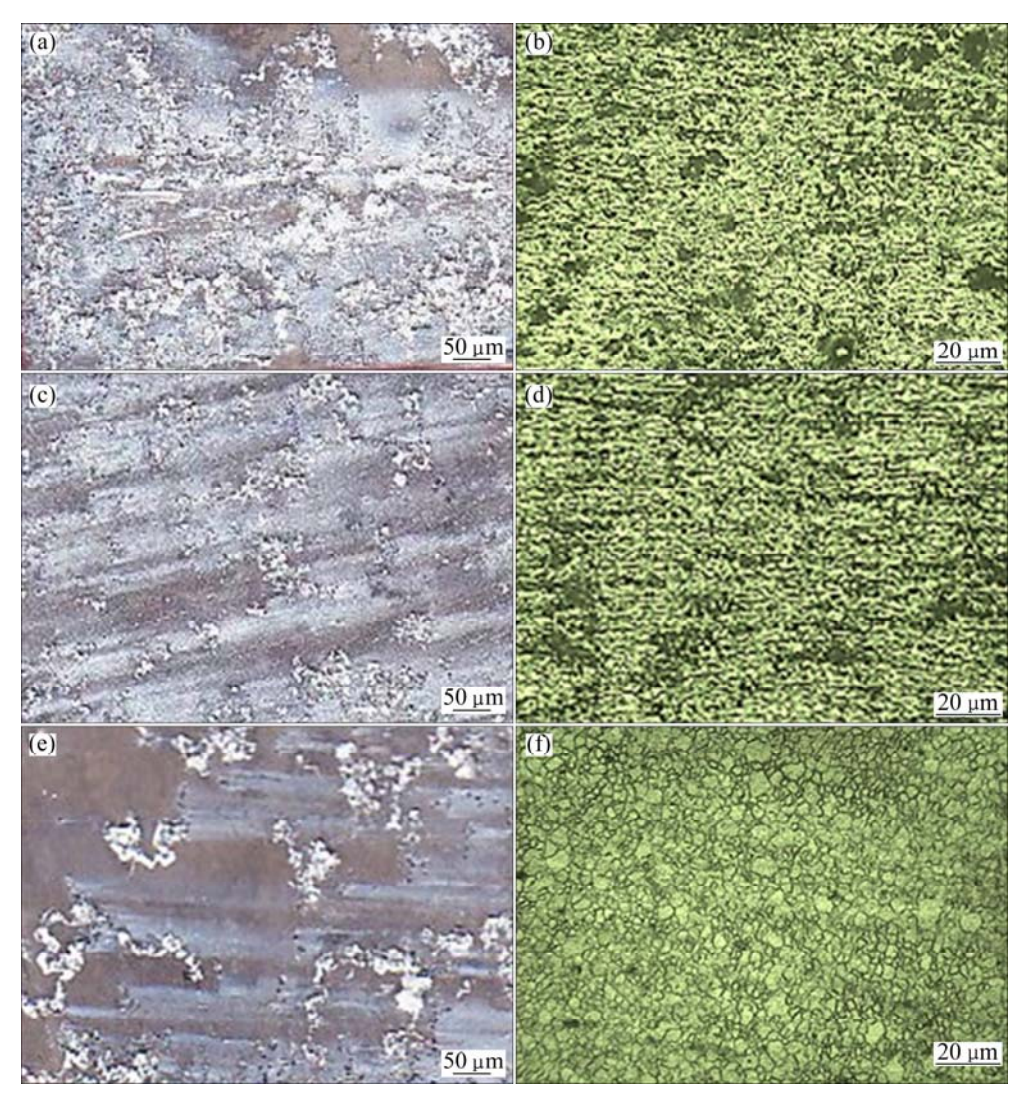


Fig. 5 Effect of pH on corrosion morphology (a, c, e) and pit morphology (b, d, f): (a), (b) pH=3; (c), (d) pH=7; (e), (f) pH=11

The equilibrium pH value required for the precipitation of Mg(OH)<sub>2</sub> is around 11. Highly acidic solutions are aggressive towards magnesium, resulting in a very high corrosion rate. In Mg–Al alloys, a pH above 9 favors the formation of Mg(OH)<sub>2</sub> (depending on the concentration of the medium) [17]. From the corrosion morphology, it is seen that the more corrosion products appear in the lower pH than in the higher pH. The corrosion rate seems to be increased with the decrease in pH.

From the pit morphology of friction stir welded metal after immersion test at different pH values of 3, 7 and 11 with a constant chloride ion concentration of 0.60 mol/L and immersion time of 5 h, it is observed that the matrix shows the pitting marks and the pitting corrosion takes place at the friction stir welded microstructure. The particles are Mg–Al compound and fragmented Mg<sub>17</sub>Al<sub>12</sub>. The number of pits is more in the welded metal region when it is immersed in the solution of low pH. Hence, the corrosion rate increases with the decrease in pH value.

Since the increase of grain and grain boundary in the weld metal region, the grain boundary acts cathode, causing micro galvanic effect. Corrosion tends to be concentrated in the areas adjacent to the grain boundary until eventually the grain may be undercut and fall out. It means that pH value is one major factor on corrosion rate.

Figure 6 shows the corrosion morphology and pit morphology of the corrosion test specimen after immersion tests at different chloride ion concentrations of 0.2, 0.6 and 1.0 mol/L with constant pH 7 and immersion time of 5 h, respectively. The increase in corrosion rate with increasing chloride ion concentration is attributed to the participation of chloride ions in the dissolution reaction. Chloride ions are very aggressive to magnesium. The adsorption of chloride ions to oxide covered magnesium surface transforms Mg(OH)<sub>2</sub> to easily soluble MgCl<sub>2</sub> [17]. It is considered that the corrosion becomes severe owing to the penetration of hydroxide film by Cl<sup>-</sup> ion and thereby the formation of

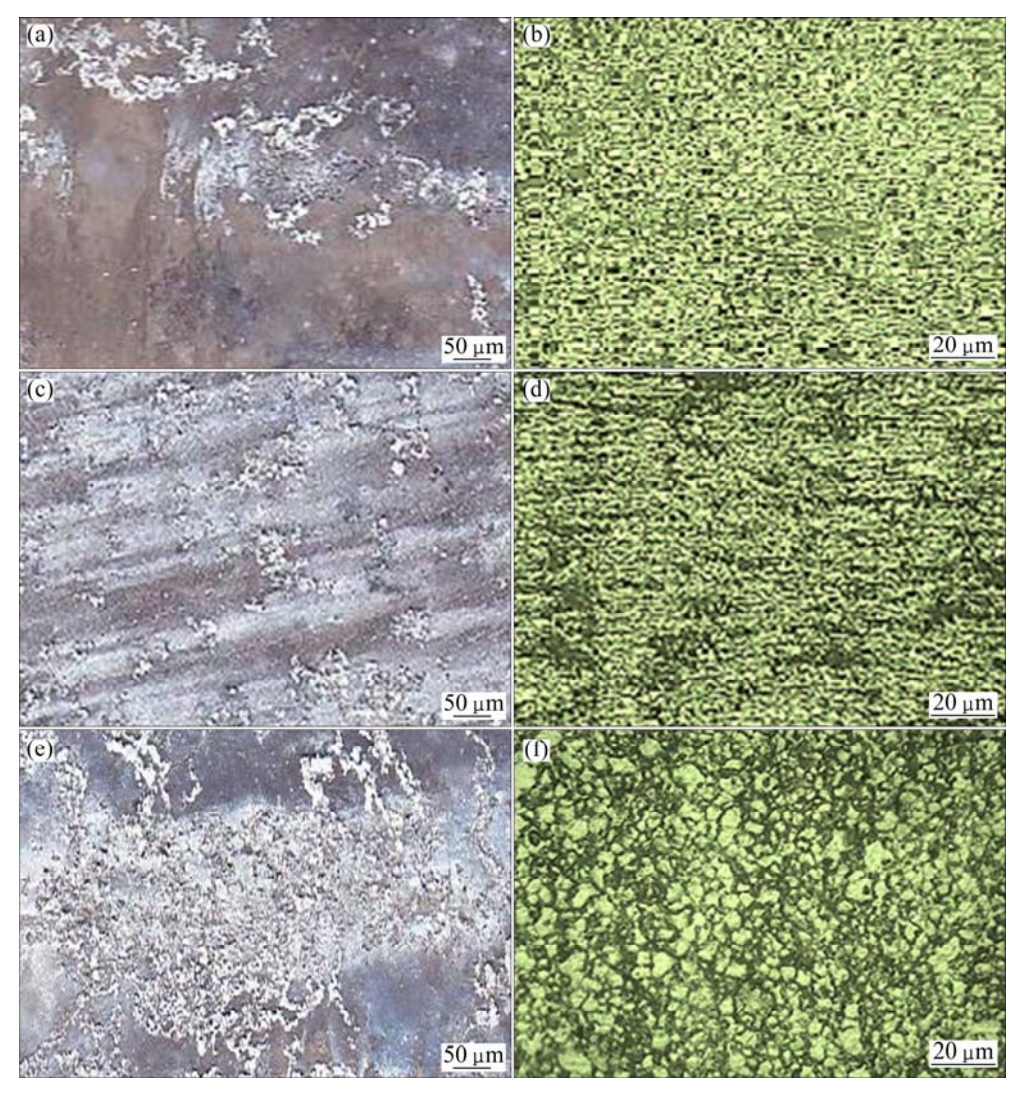


**Fig. 6** Effect of chloride ion concentration on corrosion morphology (a, c, e) and pit morphology (b, d, f): (a), (b) 0.2 mol/L; (c), (d) 0.6 mol/L; (e), (f) 1.0 mol/L

metal hydroxyl chloride complex governs the following reaction,

$$Mg^{2+} + 2OH^{-} + 2CI^{-} \rightarrow 2Mg(OH)_{2}Cl_{2}$$
 (12)

This corrosion behavior is consistent with the current understanding that the corrosion behavior of magnesium alloys is governed by a partially protective surface film with the corrosion reaction occurring predominantly at the breaks or imperfections of the partially protective film [24].

Figure 7 shows the corrosion morphology and pit morphology of the corrosion test specimen after immersion tests at immersion time of 1 h, 5 h and 9 h with constant pH 7 and chloride ion concentration of 0.60 mol/L, respectively. The corrosion rate is decreased with increasing immersion time. It proves that the initial corrosion product impedes the passage of corrosion medium and provides protection for the metal

substrate. In long-time immersion with magnesium dissolution and hydrogen evolution, the pH value of the solution will increase, namely basification. Basification should be propitious to the formation of passive film, which can protect the alloy [25]. The insoluble corrosion products on the surface of alloy could slow down the corrosion rate.

Furthermore, from the pit morphology, the grain is refined and quite lots of  $\beta$  particles distribute continually along the grain boundary. In this case,  $\beta$  phase particles cannot be easily destroyed and, with the increase of corrosion time, the quantity of  $\beta$  phases in the exposed surface would increase and finally  $\beta$  phases play the role of a corrosion barrier [26]. Although there are some grains of  $\alpha$  phase still being corroded, most of  $\alpha$  phase grains are protected under the  $\beta$  phase barrier. So the corrosion rate would be decreased with increasing the immersion time.

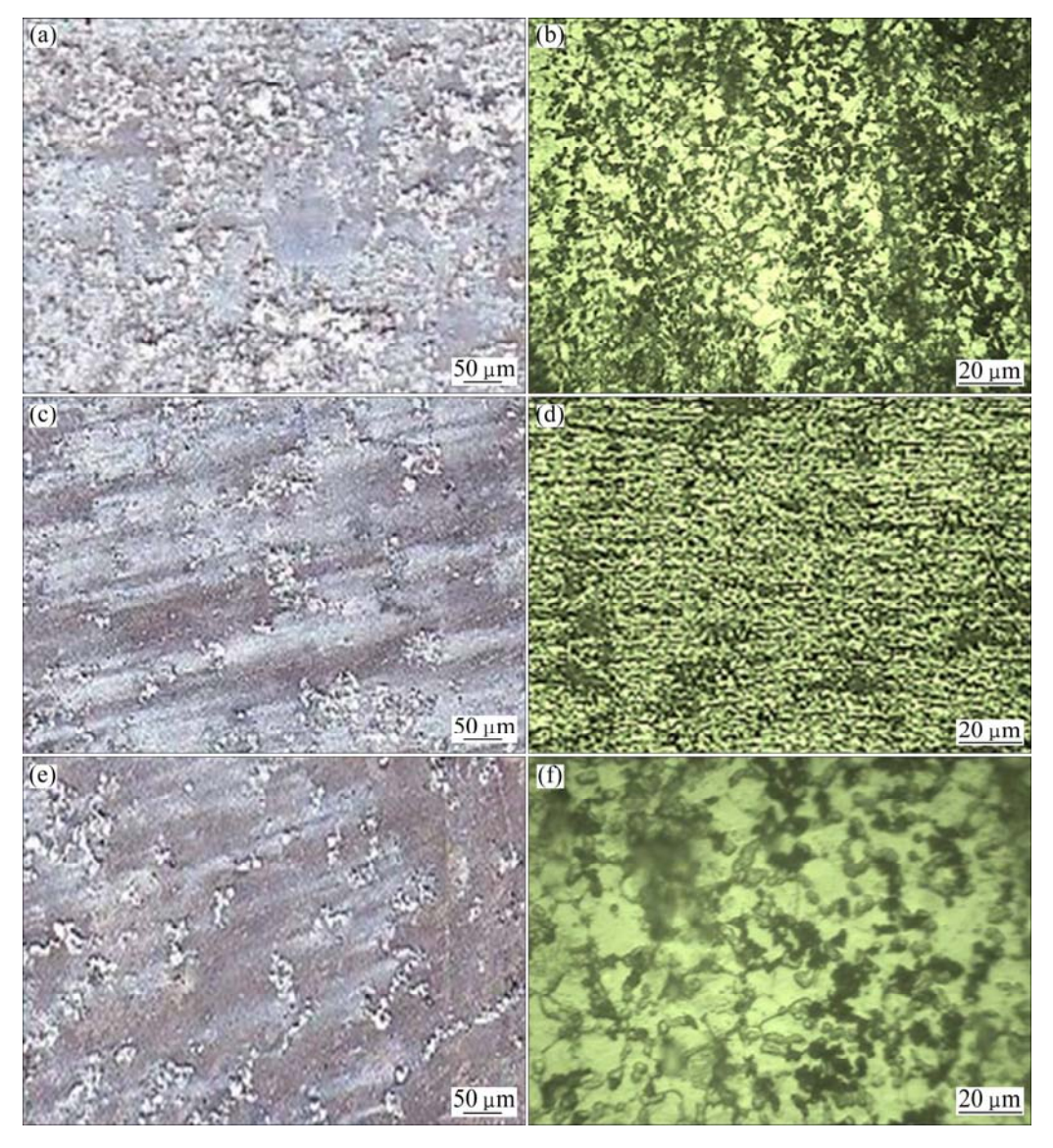


Fig. 7 Effect of immersion time on corrosion morphology (a, c, e) and pit morphology (b, d, f): (a), (b) 1 h; (c), (d) 5 h; (e), (f) 9 h

#### **5 Conclusions**

- 1) The corrosion behavior of friction stir welded AZ61A magnesium alloy welds was explored under immersed conditions in NaCl solution.
- 2) An empirical relationship was developed to predict the corrosion rate of friction stir welded AZ61A magnesium alloy welds at a 95% confidence level. The relationship was developed by incorporating the effect of pH value, immersion time and chloride ion concentration.
- 3) At all pH values, the friction stir welded metal exhibited a rise in corrosion rate with decrease in pH value. In the neutral pH, the corrosion rate remained constant approximately and a comparatively low corrosion rate was observed in alkaline solutions. The influence of pH was higher at higher concentration of chloride ion as compared to lower concentrations of neutral or alkaline solutions.
- 4) The increase in corrosion rate with increasing chloride ion concentration was attributed to the participation of chloride ions in the dissolution reaction. Chloride ions were very aggressive towards magnesium. The adsorption of chloride ions to oxide covered on magnesium surface transforms  $Mg(OH)_2$  to easily soluble  $MgCl_2$ .
- 5) The corrosion rate was decreased with the increase in immersion time. It resulted in the increase of hydrogen evolution with increasing the immersion time, which tended to increase the concentration of OH<sup>-</sup> ions thereby increasing fraction of the surface, which is the insoluble corrosion products. The insoluble corrosion products on the surface of the alloy could slow down the corrosion rate.

#### Acknowledgements

The authors would like to thank sincerely to the Department of Manufacturing Engineering, Annamalai University, Annamalai Nagar, for extending the facilities of Material Testing Laboratory to carry out this investigation. The authors are ever grateful to CEMAJOR (Centre for Materials Joining & Research), Department of Manufacturing Engineering, Annamalai University, Annamalai Nagar, for extending the facilities of corrosion testing laboratory to carry out the investigation.

# References

- MAJUMDAR J D, GALUN R, MORDIKE B, MANNA I. Effect of laser surface melting on corrosion and water resistance of a commercial magnesium alloy [J]. Material Science Engineering A, 2003, 361: 119–129.
- [2] BLAWERT C, MORALES E D, DIETZEL W, KAINER K U.

- Comparison of corrosion properties of squeeze cast and thixo-cast Mg-Zn-RE alloys [J]. Materials Science Forum, 2005, 488-489: 697-700
- [3] FONTANA M G. Corrosion principles [M]//FONTANA M G. Corrosion Engineering. Boston: McGraw-Hill, 1986: 12–38.
- [4] MAKAR G L, KRUGER J. Corrosion of magnesium [J]. International Materials Review, 1993, 38: 138–153.
- [5] SONG G, ATERNS A. Understanding magnesium corrosion—A frame work for improved alloy performance [J]. Advanced Engineering Materials, 2003, 5: 837–858.
- [6] SHAW B A. Corrosion resistance of magnesium alloys [M]//KORB L J. ASM Handbook. Vol. 13A: Corrosion. Ninth edition. Metals Park: ASM International Handbook Committee, 2003: 692.
- [7] XU Wei-feng, LIU Jin-he, ZHU Hong-qiang. Pitting corrosion of friction stir welded aluminium alloy thick plate in alkaline chloride solution [J]. Electrochimica Acta, 2010, 55: 2918–2923.
- [8] ASTM G31—72. Standard practices for laboratory immersion corrosion testing of metals [S]. 2004.
- [9] AVEDESIAN M M, BAKER H. Magnesium and magnesium alloys[M]. Materials Park: ASM International, 1999: 194–210.
- [10] GAO Li-li, ZHANG Chun-hong, ZHANG Mi-lin, HUANG Xiao-mei, SHENG Nan. The corrosion of a novel Mg-11Li-3Al-0.5RE alloy in alkaline NaCl solution [J]. Journal of Alloy Compounds, 2009, 468: 285–289.
- [11] INOUE H, SUGAHARA K, YAMAMOTO A, TSUBAKINO. Corrosion rate of magnesium and its alloys in buffered chloride solution [J]. Corrosion Science, 2002, 44: 603-610.
- [12] SONG G, ATRENS A, DARGUSCH M. Influence of microstructure on the corrosion of die cast AZ91D [J]. Corrosion Science, 1999, 41: 249–273.
- [13] ZENG Rong-chang, ZHANG Jin, HUANG Wei-jiu, DIETZEL W, KAINER K U, BLAWERT C, WEI K E. Review of studies on corrosion of magnesium alloys [J]. Transactions of Nonferrous Metals Society of China, 2006, 16: s763-s771.
- [14] HOLLY MARTIN J, HORSTE MEYER M F, PAUL WANG T. Structure property quantification of corrosion pitting anodes immersion and salt spray environment on an extruded AZ61 magnesium alloy [J]. Corrosion Science, 2011, 53: 1348–1361.
- [15] BALASUBRAMINAN P, ZETLER R, BLAWERT C, DIETZEL W. A study on the effect of plasma electrolytic oxidation on the stress corrosion cracking behavior of wrought AZ61 Mg alloy and its friction stir welding [J]. Material and Characteristics, 2009, 60: 289–389.
- [16] ZENG Rong-chang, CHEN Ju-ro, DIETZEL W, ZETTLER R, DOS SANTOS J F. Corrosion of friction stir welded magnesium alloy AM50 [J]. Corrosion Science, 2009, 51: 1738–1746.
- [17] ALTUN H, SEN S. Studies on the influence of chloride ion concentration and pH on the corrosion behavior of AZ63 magnesium alloy [J]. Materials and Design, 2004, 25: 637–643.
- [18] SONG Ying-wei, SHAN Da-yong, CHEN Rong-shi, HAN En-hou. Effect of second phases on the corrosion behavior of wrought Mg-Zn-Y-Zr alloy [J]. Corrosion Science, 2010, 52: 1830-1837.
- [19] GOH K H, LIM T T, CHUI P. Evaluation of the effect of dosage, pH and contact time on high-dose phosphate inhibition for copper corrosion control using response surface methodology (RSM) [J]. Corrosion Science, 2008, 50: 918–927.
- [20] BALASUBRAMANIAN V, GUHA B. Fatigue life prediction of load carrying cruciform joints of pressure vessel steel by statistical tools [J]. Materials and Design, 2004, 25: 615–623.
- [21] RAJAKUMAR S, MURALIDHARAN C, BALASUBRAMANIAN V. Predicting tensile strength, hardness and corrosion rate of friction stir welded AA6061-T<sub>6</sub> aluminum alloy joints. [J]. Materials and Design, 2011, 32: 2878–2890.
- [22] SHI Zhi-ming, LIU Ming, ATRENS A. Measurement of Corrosion

- rate of magnesium alloys using Tafel extrapolation [J]. Corrosion Science, 2010, 52: 579–588.
- [23] ZHAO Ming-chun, LIU Ming, ATRENS A. Influence of pH and chloride ion concentration on the corrosion of Mg alloy ZE41 [J]. Corrosion Science, 2008, 50: 3168–3178.
- [24] CHENG Ying-liang, QIN Ting-wei, WANG Hui-min, ZHANG Zhao. Comparison of corrosion behavior of AZ31, AZ91, AM60 and ZK60
- magnesium alloy [J]. Transactions of Nonferrous Metal Society of China, 2009, 19: 517-527.
- [25] SONG Guang-ling. Corrosion and protection of magnesium alloy [M]. Beijing: Chemical Industries Press, 2006: 75–84. (in Chinese)
- [26] SONG Ying-wei, SHAN Da-yong, CHEN Rong-shi, HAN En-hou. Corrosion characterization of Mg-8Li alloy in NaCl solution [J]. Corrosion Science, 2009, 51: 1087–1094.

# AZ61A 镁合金搅拌摩擦焊接头在 NaCl 溶液中的腐蚀行为

# A. DHANAPAL<sup>1</sup>, S. RAJENDRA BOOPATHY<sup>2</sup>, V. BALASUBRAMANIAN<sup>3</sup>

- $1.\ Department\ of\ Mechanical\ Engineering,\ Sri\ Ramanujar\ Engineering\ College,\ Vandalur,\ Chennai-600048,\ Tamil\ Nadu,\ India;$ 
  - 2. Department of Mechanical Engineering, College of Engineering, Guindy,

Anna University, Chennai - 600 025, Tamil Nadu, India;

- 3. Center for Materials Joining & Research (CEMAJOR), Department of Manufacturing Engineering, Annamalai University, Annamalainagar 608 002, Chidambaram, Tamil Nadu, India
- 摘 要:对 6 mm 厚的挤压态 AZ61A 镁合金板进行搅拌摩擦对接焊。采用浸泡试验研究焊接接头在 NaCl 溶液中的腐蚀行为,建立了一个经验公式来预测在不同的溶液 pH 值、浸泡时间和氯离子浓度下的接头腐蚀速率。该经验公式的可信度水平为 95%。采用 3 因素、5 水平的中央复合旋转设计方法来减少实验工作量。采用响应面方法来构建方程。结果表明,在碱性溶液中 AZ61A 镁合金接头的腐蚀速率要比其在酸性或中性溶液中的低,而且腐蚀速率随着氯离子浓度的降低和浸泡时间的延长而减少。 $\beta$  相的分布对其腐蚀形貌有重要影响。

关键词: 镁合金; 浸泡腐蚀; 搅拌摩擦焊

(Edited by YUAN Sai-qian)